

Research on Enhancing Vehicle Fuel Efficiency Based on Custom Material Properties

Qingzhuo Li

*College of Automotive Engineering, Jilin University, Changchun, China
13083778808@163.com*

Abstract. This paper highlights the benefits of using carbon fiber, ceramics, titanium alloys, and aluminum alloys to replace traditional metals in the manufacture of automotive components. Carbon fiber is lightweight and of high strength and has a high impact absorption capacity. Its wide application will significantly reduce the weight of the vehicle, but there is a problem of high cost. Ceramics are hard and wear-resistant and can be used to manufacture parts that are directly subjected to alternating loads. Titanium alloy has high hardness but high density and can be used to manufacture key parts with high strength requirements. The aluminum alloy has high specific strength, but low fatigue strength and no wear resistance, so it can be used to manufacture parts that do not bear alternating loads such as frames. Furthermore, these materials possess a significantly lower density compared to conventional steel. They are reasonably applied to the manufacture of automotive parts, to ensure safety the same time can also significantly improve fuel efficiency.

Keywords: Fuel efficiency, Carbon Fiber, Ceramic, Titanium Alloy, Aluminum Alloy

1. Introduction

Improving fuel efficiency has long been a crucial metric for consumers to evaluate the affordability of vehicle options and is a common topic for environmental conservation efforts. As a result, many countries around the globe are pushing industries to reduce emissions that are harmful to the environment [1-4]. Several factors, including aerodynamic drag, power transmission efficiency, engine performance, and much more can influence fuel efficiency. One of the most impactful ways to increase fuel efficiency is to reduce the weight of components in the vehicle assembly [1]. This can be accomplished by optimizing the material selection for every individual component of the vehicle. Emerging fabrication and manufacturing technologies are now enabling the creation of materials with custom properties. This means that instead of engineers selecting from available materials, they are exploring new frontiers and inventing complex materials such as Carbon Fiber, Ceramic, Titanium Alloy, and Aluminum Alloy, with the desired properties throughout the vehicle, while upholding standards for a safe consumer product. Both specific strength and fatigue resistance play significant roles in improving vehicle fuel efficiency. The enhancement of specific strength contributes to vehicle lightweighting, which directly reduces fuel consumption. Meanwhile, the improvement of fatigue resistance ensures the safety and durability of vehicle structures, indirectly enhancing fuel efficiency.

Fatigue resistance refers to the highest stress test cycle of a material or product before failure occurs, after multiple specified maximum stress test cycles. With the development of technology, various industries have replaced manual labor with machines, which requires extremely high precision for machines. This has also brought new challenges to manufacturers: how to choose materials with high fatigue resistance, good toughness, and high hardness to manufacture machines. To solve these challenges, researchers need to conduct multiple tests, experiments, and calculations to identify the most suitable materials for manufacturing machines to help people solve practical problems [5-9]. In automobile design and manufacturing, improving the fatigue resistance of materials can significantly enhance the structural strength and durability of automobiles, thereby reducing accidents caused by material fatigue fracture and ensuring driving safety. For example, the valve spring in a car engine needs to have high fatigue resistance to ensure that it will not break due to fatigue during long-term operation, thereby maintaining the normal operation of the engine [10]. This high fatigue resistance material can significantly improve maneuverability and fuel economy, as it can reduce performance degradation caused by material fatigue and maintain efficient engine operation.

Specific strength refers to the ratio of the tensile strength and the density of the material, it is an important standard for deciding the strength of a material compared to its weight. In the design of cars, specific strength is crucial for improving fuel utilization efficiency. High specific strength can make sure to decrease the weight of cars while keeping the same vehicle structural strength, increasing the efficiency of cars by decreasing weight [11-13]. Recently, researchers have been doing tests, calculations, and experiments to improve specific strength.

This paper will review the literature and analyze the content related to the specific strength and fatigue resistance of four customized materials: carbon fiber, ceramics, titanium alloy, and aluminum alloy. After the analysis, it will be determined that carbon fiber composites are the best choice for lightweight automotive materials to improve fuel efficiency.

2. Discussion

2.1. Carbon Fiber

Carbon Fiber (CF) composites are materials consisting of carbon fibers, shown in Figure 1, embedded or dispersed within a matrix material, typically a polymer, ceramic, or metal. CF stands as a unique fiber category, primarily consisting of carbon elements, with varying carbon concentrations depending on its type, typically exceeding 90% in most varieties. The arrangement of CF in CF composites can be unidirectional, bidirectional, or multidirectional, depending on the intended application and desired properties. Carbon Fiber (CF) composites possess several notable physical properties, including excellent fatigue resistance, high specific strength, thermal stability, and corrosion resistance. Its versatility extends to various industries including aerospace, automotive, energy, sports, and recreation, where its use often results in significant weight reduction and performance enhancement, as shown in Figure 2.

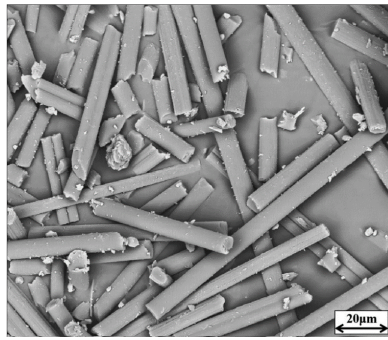


Figure 1. FESEM of the as-received short carbon fiber. FESEM, field emission scanning electron microscope [14]

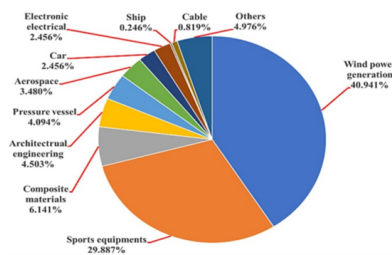


Figure 2. China's CFRPs application ratio in 2020 [15]

One common problem is that carbon fibers possess a certain degree of fatigue resistance, but it is not sufficient for their application in automobiles. Carbon fiber composites are put into use to solve this problem. Among them, Carbon Fiber/Polyphenylene Sulfide (CF/PPS) laminate can enhance the fatigue resistance. They were manufactured using a semi-industrial hydraulic press via hot compression molding. A specific processing cycle studied and established in prior work, shown in Figure 3, was followed, involving stacking 9 layers of CF/PPS semi-pregs, heating to 300°C with increasing force, holding for 30 minutes, and then cooling to room temperature. The entire process took approximately 90 minutes per laminate [5]. An investigation was carried out on the fatigue resistance of composite Grivory GCL-4H, which comprises a semi-crystalline polyamide stabilized against heat, augmented with a partially aromatic polyamide component, and reinforced with elongated carbon fibers [6].

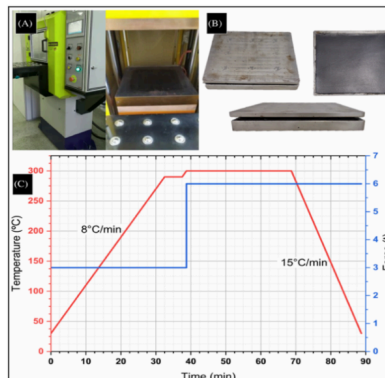


Figure 3. (A) Press used in the processing, (B) the system consisting of the aluminum mold and the semipreg layers, and (C) the processing cycle used in the preparation of CF/PPS laminates [5]

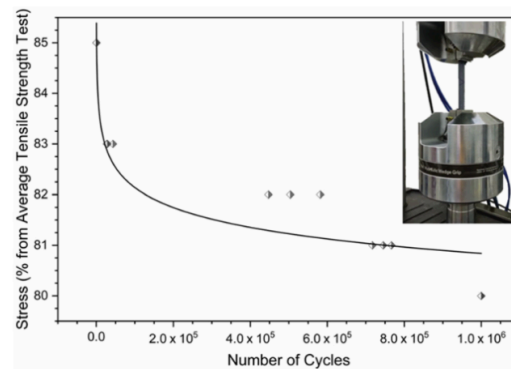


Figure 4. S–N curve for CF/PPS composite obtained after the fatigue test [5]

The CF/PPS composites demonstrated a robust elastic modulus of approximately 37.2 GPa with a narrow range of 0.2 GPa, alongside an average tensile strength of 800 MPa, accompanied by a margin of error of 73 MPa. Furthermore, these composites exhibited impressive durability, enduring 1 million fatigue cycles without failure when tested at 80% of their maximum stress level [5], shown in Figure 4. Furthermore, regarding long carbon fiber-reinforced polyamide, an examination was conducted to assess the impact of varying extraction angles (0° , 30° , 45° , and 90°) from a plate on its fatigue lifespan. The study unveiled a significant sensitivity in fatigue behavior to the alignment between the loading axis and the melt flow axis. Specifically, the samples displayed optimal properties when oriented precisely parallel (0°) to the melt flow direction, with a progressive decrease in performance as the angle of orientation deviated towards 90° [6], as shown in Figure 5. The study underscores the appropriateness of CF/PPS composites for high-strength, weight-saving automotive applications, underscoring their capacity to contribute significantly to the manufacture of long-lasting and high-performance components. The exceptional fatigue endurance, robust mechanical attributes, and featherweight characteristics of CF/PPS composites render them highly suitable for stringent automotive applications. This research endeavors to propel the field of materials engineering forward and enhance the design optimization of automotive components.

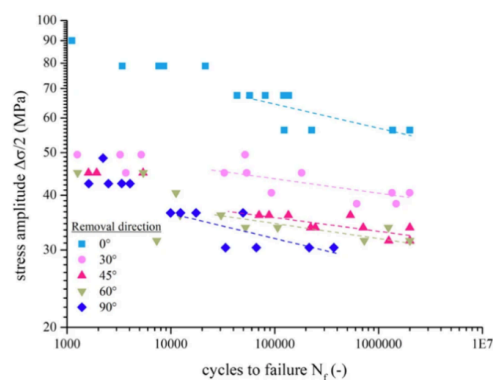


Figure 5. Results of fatigue tests tested at $f = 10$ Hz, $R = 0.1$, and $T = RT$ with SS (small specimens) \times samples. Influence of different removal directions [6]

A common problem is that some materials, such as sucrose-derived carbon foams and syntactic foams (Figure 6), are lightweight but possess relatively low compressive strength or shear strength [5,6], which leads to the fact that the specific strength of these materials has not been significantly improved. To solve this, milled carbon fibers and chopped carbon fibers were added as

reinforcement. Sucrose and CF were mixed, ball-milled, and then thermo-foamed in molten sucrose. The resulting foam was dehydrated and carbonized to obtain the final carbon composite foam [11]. Using phenolic microspheres as the core material, phenolic resin as the binder, and a minor inclusion of chopped carbon fibers, fiber-reinforced syntactic foams were successfully synthesized [12]. Mechanical properties were tested using SEM, a universal testing machine, and XRD.

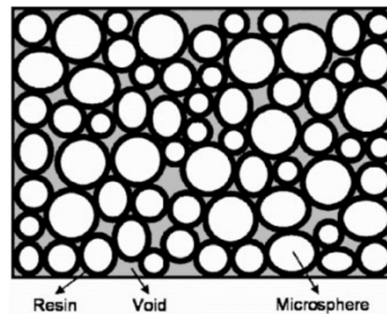


Figure 6. Schematic morphology of typical syntactic foam [12]

At a carbon fiber (CF) length of 33 micrometers and a concentration of 2 weight percent, the composite foams exhibited peak values for both density and specific compressive strength. When compared to the unreinforced foam, an enhancement of up to 125 percent in compressive strength and 92 percent in specific compressive strength was attained. Notably, CF lengths shorter than 33 micrometers resulted in a decline in strength, which can be attributed to a diminished aspect ratio that hindered effective stress transfer within the composite structure [5]. The specific strength values for both the P-type foams (depicted in Figure 7) and the unreinforced foams are presented in Figure 8. In comparison to the unreinforced foams, the P-type foams demonstrated a notably superior specific strength under compression, tension, and shear loading conditions. Notably, the P-type foams with a density of 350 kg/m³ exhibited the highest specific strength in both compression and tension, whereas the P-type foams of a lower density, specifically 250 kg/m³, demonstrated the greatest specific strength in shear [12]. The enhancement in mechanical performance was credited to the efficient stress distribution and homogeneous dispersion of carbon fibers (CFs). The incorporation of CF reinforcement significantly bolstered the mechanical characteristics of phenolic microsphere syntactic foams, with a pronounced impact on P-type foams. This methodology holds promise for the fabrication of composite syntactic foams that possess exceptional specific strength, making them suitable candidates for utilization as core materials in sandwich structures.

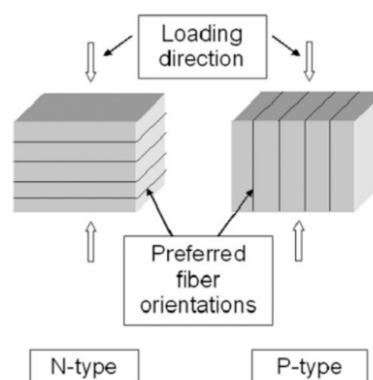


Figure 7. Definition of P-type and N-type foams [12]

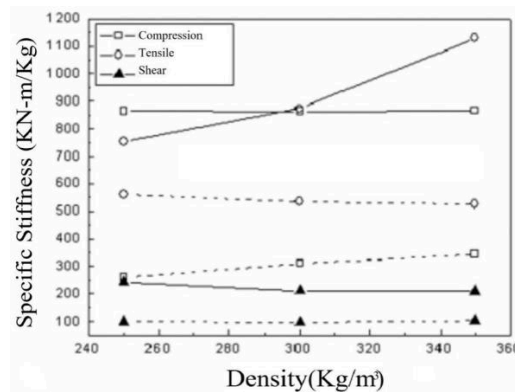


Figure 8. Specific strength for the P-type foams and the neat foams. The bold solid lines are the lines for the P-type foams and the dash lines are the lines for the neat foams [12]

2.2. Ceramic

A ceramic is a solid material formed by sintering non-metallic mineral materials such as clay, quartz, and feldspar at high temperatures. It typically has good hardness, wear resistance, and chemical stability. There is a wide variety of ceramics, including traditional ceramics (such as pottery, porcelain, and brick) and advanced ceramics (such as electric ceramics which can be used to produce capacitors, insulating materials, sensors, and piezoelectric devices, structural ceramics which can be used to produce cutting tools, construction materials (Figure 9) and wear-resistant components, and bioceramics which can be used to produce dental implants, bone repair materials and bionic joints) [16]. Ceramics have some basic properties which are listed in Table 1. In the automotive manufacturing industry, ceramics are often used to replace heavy metal materials for producing wear-resistant components like brake pads and cylinder liners. By doing so, the overall weight of the vehicle is diminished, resulting in enhanced fuel efficiency.



Figure 9. A type of ceramic tile

Table 1. Basic properties of ceramics

Basic Properties	Description
High-Temperature Resistance	Ceramics have good high temperature resistance and are suitable for high temperature environments.
Insulation	Most ceramic materials have good electrical insulation properties and are therefore commonly used in the manufacture of electronic components.

Table 1. (continued)

Corrosion Resistance	Ceramics have good resistance to chemicals and are not easily damaged by chemical reactions.
High Hardness	Ceramic materials are usually very hard and not easily scratched.

One of the most important methods of manufacturing ceramics is Chemical Vapor Deposition. Four kinds of typical reactors used in chemical vapor deposition are shown in Figure 10.

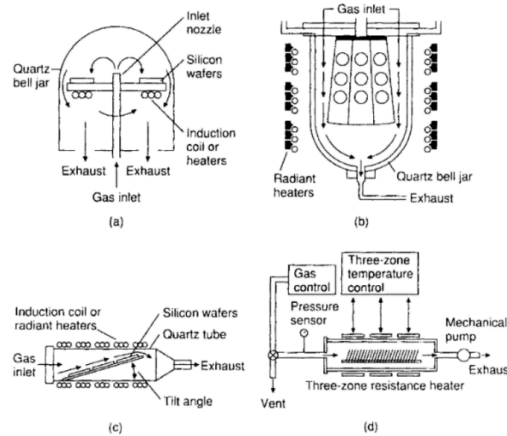


Figure 10. 2Typical reactors used in chemical vapor deposition: (a) pancake reactor; (b) barrel reactor; (c) horizontal reactor; (d) low-pressure (LPCVD) reactor [16]

To assess the durability under cyclic loads of a novel translucent zirconia material, a study by Heintze et al. employed circular specimens crafted from the material and machined eighteen 3-unit fixed partial dentures intended for the replacement of the upper first molar on a precision 5-axis milling apparatus. These FPDs featured a connector dimension of 4 mm x 4 mm, as depicted in Figure 11. In a separate investigation, Guangming Zheng et al. delved into the mechanical behavior and microstructural characteristics of Sialon-Si₃N₄ gradient composite ceramic materials synthesized via hot pressing. They subjected the ceramic samples to grinding, polishing, and three-point bending tests. Additionally, they utilized a scanning electron microscope (SEM, JSM-6380LA, Japan) to inspect the fractured surfaces of the composites after gold coating, providing insights into their microstructure. The thermal shock resistance of the materials was evaluated by exposing them to seven distinct temperature differentials (ΔT) ranging from 200 °C to 800 °C, with intervals of 100 °C, then measuring their flexural strength after each test.

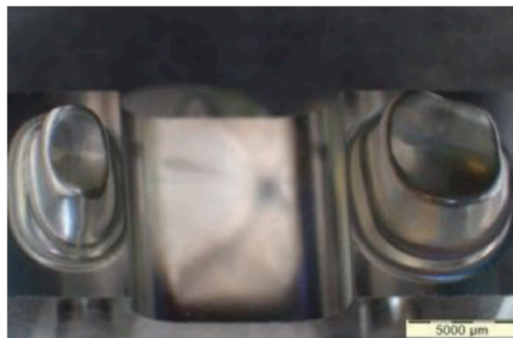


Figure 11. PMMA Tooth Model (replacement of first upper molar) [7]

Heintze et al. found that the maximum allowable principal stress (max) of the IPS e.max ZirCAD MT3, which does not lead to failure, ranged between 208 MPa and 223 MPa. The maximum fatigue strength of the IPS e.max presses at 2×10^6 cycles ranged between 78 and 90 MPa [7]. Given the potential limitations of a single load-to-fracture test in accurately assessing the durability of dental restorations, a more comprehensive fatigue testing protocol that simulates the millions of chewing cycles encountered in real-world use is warranted. Notably, zirconia molar bridges have demonstrated superior fatigue resistance compared to their lithium disilicate counterparts. Consequently, zirconia emerges as a more favorable material choice for fixed partial dentures (FPDs), offering enhanced durability and longevity over lithium disilicate. The research conducted by Zheng et al. revealed that the graded ceramic composites possessed superior flexural strength in comparison to their homogeneous counterparts across all ranges of thermal shock temperature variations, as depicted in Figure 12. This enhanced mechanical performance of the graded materials is attributed to their intricate interplay of reinforcing and toughening mechanisms. Furthermore, a notable aspect is the development of compressive residual stresses within the surface layer of these graded ceramics. These compressive stresses effectively counteract the tensile stresses induced during thermal shock, thereby contributing to the overall robustness of the material.

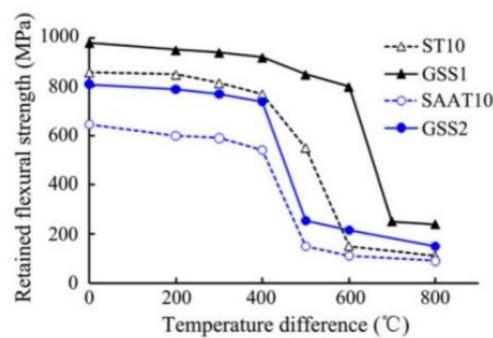


Figure 12. The ability to maintain flexural strength across varying temperature differentials after a single thermal shock exposure [17]

For ceramic materials, there are mutual constraints between some physical properties and strength, such as toughness and strength, porosity, and strength. High strength leads to low toughness, and high toughness leads to low strength. Excessive porosity reduces the weight of the material while at the same time leading to very low mechanical properties of the ceramic. However, practical needs are often demanding, which requires us to create materials with both high specific strength and high toughness, high porosity, and high density. Incorporating a metal or polymer as a secondary phase within the micro-lattice framework allows for the creation of composite materials that can harness the strengths of both constituents. These composites, characterized by two distinct and interconnected phases, are termed interpenetrating phase composites. For this investigation, we have opted to model the truss lattice structure using Bravais lattices with BCC (body-centered cubic) and SC (simple cubic) configurations, as depicted in Figure 13. Notably, the diameters of the struts in these lattice structures were specified at 0.852 mm for BCC and 1.3 mm for SC, respectively, ensuring precise simulation parameters.

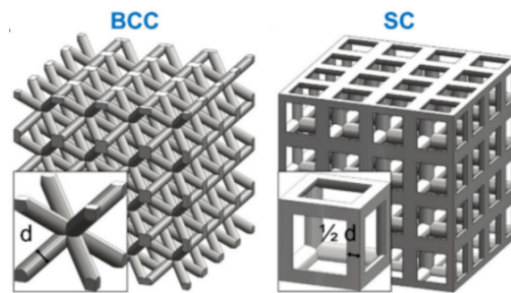


Figure 13. An overall schematic illustration of the samples and their design investigated in this work, including BCC and SC [16]

Utilizing zeolite as the primary component, we devised a method that employed particle-stabilized foaming to produce open-celled alumina foams. The characterization of these ceramic foams encompassed an analysis of their microstructure, open-cell porosity, and mechanical attributes. A thorough examination of the mechanisms responsible for boosting compressive strength and facilitating the development of open cells was conducted, with a particular focus on fostering the adoption of open-celled ceramic foams in industrial applications. Utilizing the advanced Lithoz CeraFab 8500 3D printer from Lithoz GmbH in Austria, we successfully crafted micro-lattices made of aluminum oxide. As the polymeric filler, we employed a two-part hybrid resin system consisting of EPOLAM 2040 and its corresponding curing agent, EPOLAM 2042, sourced from Sika Ltd. in China. To evaluate the compressive properties under quasi-static conditions, we utilized a Shimadzu AG25-TB universal testing apparatus, maintaining a strain rate of 0.001 s^{-1} while documenting the deformation sequence with a digital camera. Furthermore, we developed open-celled alumina ceramic foams through a meticulous process involving the blending of various raw materials, magnetic agitation for homogenization, inverted casting for shaping, followed by heat treatment and thorough drying to ensure optimal product quality as shown in Figure 14. To simulate and analyze the structural behavior, we conducted finite element analysis using ANSYS Workbench, leveraging its explicit solver capabilities.

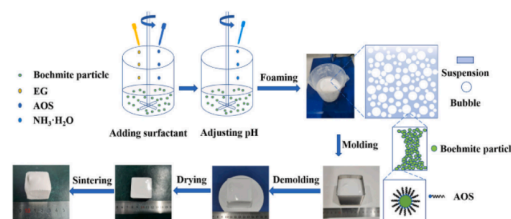


Figure 14. Schematic diagram of preparing the procedure for alumina ceramic foams [18]

In the study conducted by Xinwei Li and their colleagues, it was revealed that the interpenetrating phase composite (IPC) exhibited a remarkable 65% enhancement in strength over the mere linear summation of its components. This superiority was accompanied by exceptional specific strength values ranging from 113.5 to 142.6 MPa per gram per cubic centimeter, as well as specific energy absorption capacities spanning 25.3 to 35.6 Joules per gram, all achieved at relatively low densities hovering around 1.8 grams per cubic centimeter (refer to Table 2 for details). Notably, the incorporation of aluminum oxide within the epoxy resin matrix significantly bolstered the fracture toughness, subsequently contributing to the overall strength enhancement. During deformation, the propagation of cracks was observed to be retarded under the protective shield of the epoxy resin, a phenomenon that was visually evident and further corroborated by fracture

morphology analysis under scanning electron microscopy. Youfei Zhang and their team discovered that alumina foams crafted from zeolite demonstrated remarkable compressive strengths of 1.54 to 10.01 MPa at an elevated porosity range of 92.3% to 96.7%. This accomplishment surpasses the compressive strengths of open-celled foams produced via alternative routes by roughly an order of magnitude, all while maintaining comparable levels of porosity. The remarkable enhancement in the compressive resilience of these aerogel-like open-celled alumina foams stems primarily from two key aspects: the simultaneous development of nearly defect-free pore channels and their terminal apertures, coupled with the strategic alignment of void spaces created by the self-compaction of raw material volumes at the far ends of these pore channels, creating efficient passageways. This novel structure effectively mitigates the adverse impacts of imperfect pore structures on the mechanical robustness of the monolithic ceramic foam, particularly those arising from imperfections in the pore openings, thereby enhancing its overall performance. Furthermore, the ultra-lightweight nature of these open-cell alumina foams, coupled with their distinctive three-dimensional interconnected pore network and exceptional mechanical attributes, renders them highly promising candidates for various practical applications, including but not limited to bone scaffolds, catalyst supports, and filtration systems [18].

Table 2. Summary of the mechanical properties of the IPCs [16]

Sample	Density (g/cm ³)	Compressive strength (MPa)	Densification strain (-)	SEA (J/g)	EAE (%)
BCC + EP	1.665 ± 0.005	104 ± 1.7	0.6 ± 0.02	27.7 ± 0.3	75 ± 1
BCCG + EP	1.743 ± 0.02	101 ± 1.3	0.59 ± 0.02	26.3 ± 0.8	76.9 ± 1
SC + EP	1.83 ± 0.02	261 ± 1.5	0.58 ± 0.03	25.3 ± 2.5	43 ± 2.5
SCG + EP	1.753 ± 0.03	199 ± 1.7	0.59 ± 0.03	35.6 ± 3.6	61 ± 3.5

2.3. Titanium alloy

Titanium alloy materials have high strength, low density, good corrosion resistance, high thermal stability, and excellent low-temperature performance, as well as low thermal conductivity and elastic modulus. It refers to various alloy metals made of titanium, aluminum, vanadium, iron, Molybdenum, niobium, aluminum, carbon, and oxygen for example. The addition of these elements can improve the strength and corrosion resistance of titanium alloys. They can also lower the phase transition temperature and raise the transition temperature. Therefore, titanium alloys are widely used in the aerospace industry, such as the manufacturing of aircraft components, as shown in Figure 15. In the automotive industry, titanium alloys are also widely used, mainly in the manufacturing of car components, as shown in Figure 16. For example, Honda Motor Company in Japan uses forged titanium connecting rods on the V6 engine of the NSX racing car, while Mitsubishi Motors uses titanium valve spring seats in the V4 engine they manufacture. In the future, people will develop low-cost and high-performance new titanium alloys and titanium alloys will be widely used in the civilian industrial field.

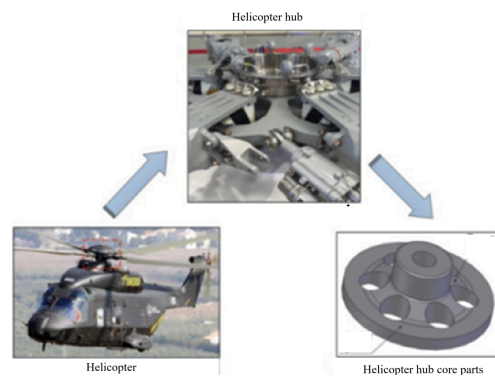


Figure 15. TB6 titanium alloy helicopter hub [8]



Figure 16. Examples of Bugatti Ti components in the automotive sector are (a) an eight-piston monobloc brake caliper (b) an active spoiler bracket and (c) tailpipe trim covers [19]

Utilizing the precise alignment of electrolyte and electrical characteristics, PEO primarily functions to generate ceramic coatings enriched with metal oxide matrices, bolstered by electrolyte additives, directly on the surfaces of valve metals and their alloys, including aluminum, magnesium, and titanium. This process occurs under the intense, momentary conditions of arc discharge-induced high temperature and pressure. While studies have indicated that plasma electrolytic oxidation (PEO) may compromise the fatigue strength of titanium alloys, the USRP processing method counters this effect by refining surface grains and introducing a compressive stress field exceeding $560 \mu\text{m}$. This treatment enhances the coating's density and minimizes surface roughness, ultimately improving the overall performance of the PEO coating. So people use ultrasonic surface rolling technology pretreatment (USRP) to alleviate this adverse effect.

Furthermore, there exist surface enhancement methodologies such as peening with shots (SPS), mechanical abrasion on the surface (MAS), and ultrasonic striking processes (USP), which significantly bolster the fatigue endurance of titanium alloys. Specifically, SPS serves as a surface fortification approach that harnesses high-velocity projectiles to bombard metallic surfaces, inducing plastic deformation and consequently generating compressive residual stresses at the surface layer of the metal. Surface mechanical wear treatment indirectly improves the fatigue resistance of titanium alloys by increasing their surface hardness and wear resistance, such as nitriding treatment, carbonization treatment, and micro-arc oxidation treatment. Ultrasonic shock treatment generates a certain degree of plastic flow on the surface of the material, causing the peaks and valleys to cancel each other out, thereby reducing surface roughness. This processing method can optimize the surface roughness of titanium alloys, thereby improving their fatigue resistance. This study conducted a test on the changes before and after adding various treatment methods to improve the fatigue resistance of titanium alloys, as shown in Figure 17 and Figure 18. In this study, the author used experimental, comparative, computational, and analytical methods to obtain results.

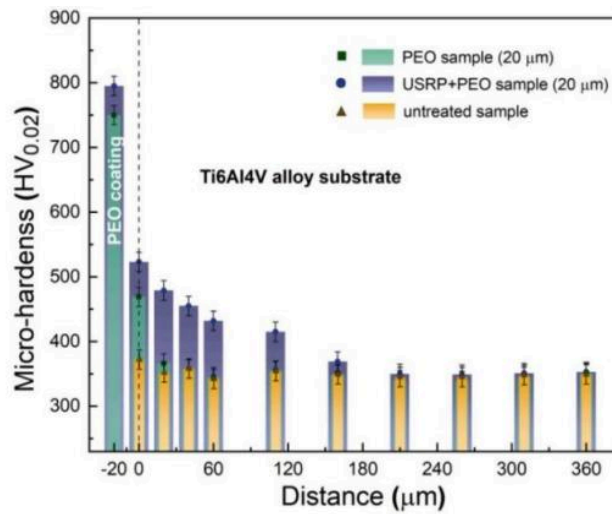


Figure 17. Cross-sectional microhardness of Ti6Al4V alloy with different surface treatments [10]

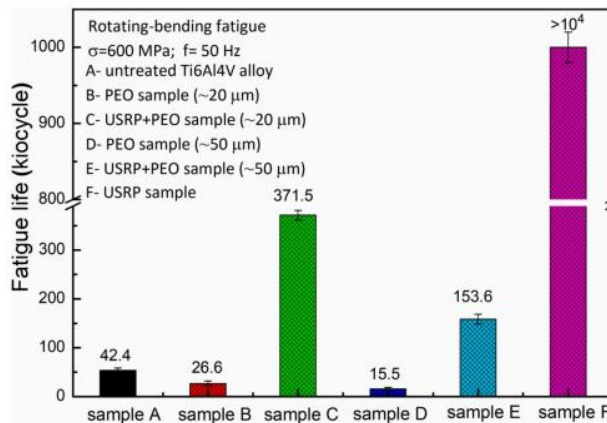


Figure 18. Fatigue life of TC4 alloy treated by different surfactants at 600 MPa [10]

The utilization of PEO coating on Ti6Al4V alloy significantly reduces its fatigue endurance, where the fatigue lifespan inversely correlates with the increased thickness of the coating. Nevertheless, pretreatment with Ultrasonic Surface Rolling (USR) process refines the surface grain structure and introduces a substantial residual compressive stress field exceeding 560 μm, which is beneficial for enhancing coating compactness, smoothing surface roughness, and ultimately improving the fatigue resistance of the specimen. As illustrated in Figure 19 and Figure 20, the Ti6Al4V alloy subjected to the combined USR-PEO technique demonstrates notably superior fatigue resistance compared to the sample solely treated with PEO. Specifically, under a 20 μm coating layer, the fatigue life of the co-strengthened sample exceeds that of the simple PEO sample by approximately 14 times at 600 MPa. The presence of the USR-strengthened layer also complicates the crack propagation path, making it more convoluted. The synergistic effect of the nanocrystalline layer at the coating/substrate interface and the compressive residual stress field on the substrate side serve as a crucial factor in enhancing the fatigue resistance of the PEO-coated sample through USR pretreatment.

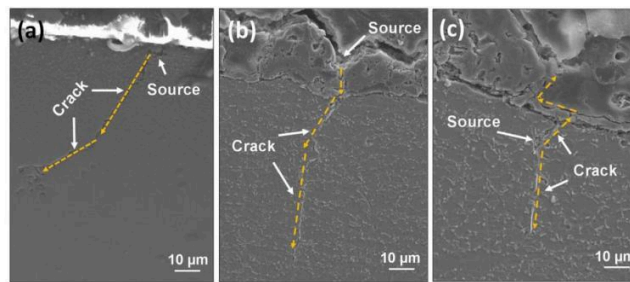


Figure 19. Crack distribution of Ti6Al4V substrate (a), PEO sample (b), and USRP-PEO co-strengthened sample (c) at the fatigue life of about 80 % under 600 MPa [10]

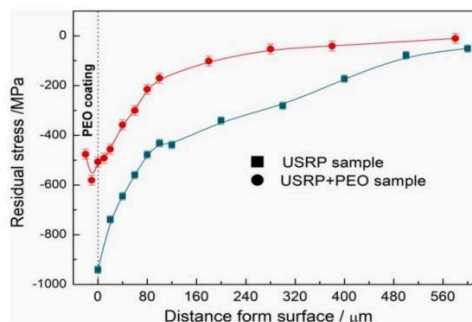


Figure 20. Residual stress distribution of Ti6Al4V alloy with different surface treatments [10]

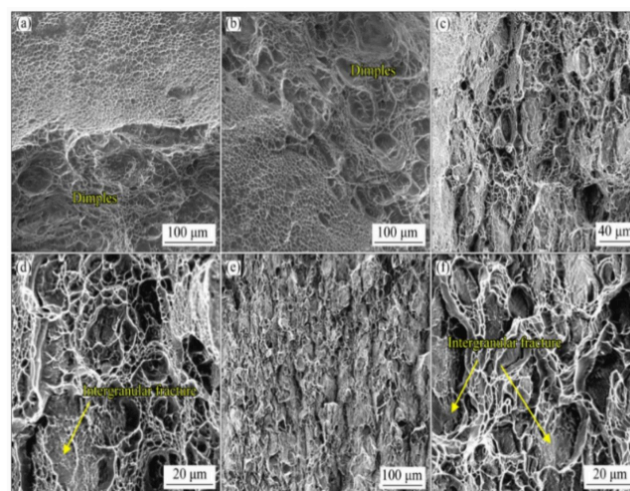


Figure 21. Morphologies of fracture surfaces: (a) Process A; (b) Process D; (c, d) Process G; (e, f) Process I [20]

The proliferation of titanium alloys in various applications, particularly in the aerospace sector, has necessitated stricter standards for component performance. As such, enhancing the strength and ductility of titanium alloys has become paramount to accommodate the relentless growth of the industry. Furthermore, precipitates within alloys, functioning as dislocation hindrances, can pose challenges, causing heightened stress concentrations and even microscopic cracks at semi-coherent interfaces due to strain mismatches. To address these issues, we propose the development of hierarchical, coherent structures grounded in metastable engineering principles. These structures feature an unprecedented density of nano-martensites, with the finest thickness reaching

approximately 22 nanometers, which remain stable even at 400°C. This innovative approach empowers cost-effective titanium alloys with exceptional strength, ductility, and fracture toughness. The hierarchical, coherent precipitation barrier (PB) strategy, leveraging nano-martensite engineering, not only surpasses the limitations of low-density micron-scale PBs in conventional titanium alloys but also fosters an abundant supply of dislocation origins and obstacles, fostering a self-sustaining hardening mechanism that harmoniously blends ultra-high strength with exceptional toughness. As the volume fraction of the secondary α phase escalates, it continually fortifies the intragranular region, thereby rendering the grain boundaries comparatively weaker. Consequently, an intergranular cleavage pattern emerges and progressively prevails on the fracture surface, as illustrated in Figure 21.

A fatigue crack initially emerges at the interface between the primary α and β phases, traversing through the α_L region and severing the thin β laths, thereby creating a direct route for the crack to propagate in the titanium alloy's microstructure (TCM). Notably, the β laths exhibit diminished resistance to crack progression when they remain unprecipitated with the secondary α phase (α_s). In contrast, the primary path of crack propagation in the fatigue-limited material (FLM) is notably irregular and convoluted. This characteristic, characterized by a heightened capacity for crack deflection and branching, effectively postpones the coalescence of cracks, as illustrated in Figure 22.

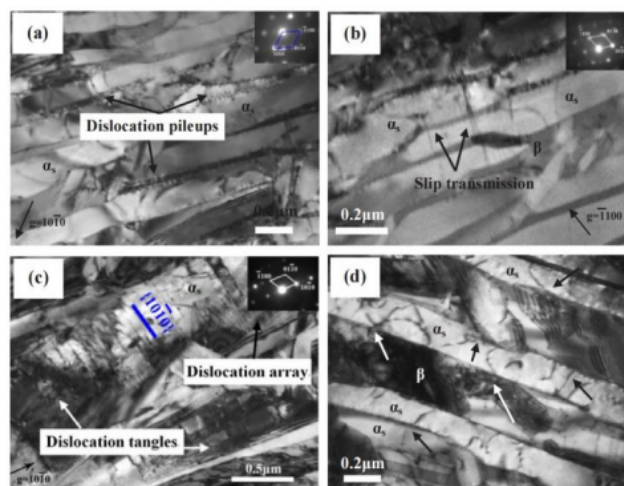


Figure 22. Dislocation evolution at various stress amplitudes: (a–b) low stress of 660 MPa, (a) some dislocation pileups at the α_s/β interface; (b) slip bands pass through the thin β lath [7]; (c–d) medium stress of 690 MPa; (c) prismatic slip bands and dislocation arrays produced in the α_s , dislocation observed in the β lath; (d) slip bands transferred through the thin β lath with increasing the stress [8]

The alternating stress applied to the surface of the PEO-coated sample typically generates multiple initiation points for fatigue cracks. However, when the Ti6Al4V alloy sample undergoes USRP pretreatment before PEO coating, a notable transformation occurs in the fatigue crack origination pattern. Instead of multiple sources, a single crack source emerges and shifts to a subsurface location, situated approximately 240 μm beneath the surface. Additionally, the presence of the USRP-strengthened layer contributes to a more intricate and convoluted crack growth trajectory, as evident in Figure 23.

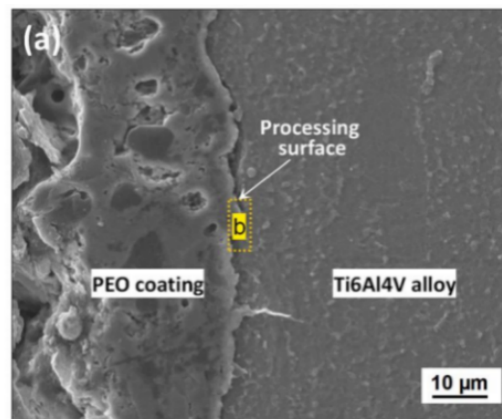


Figure 23. Cross-sectional FESEM image for USRP-PEO co-strengthened sample with PEO coating of 20 μm

2.4. Aluminum alloy

Aluminum alloy is a kind of alloy. Alloys are metallic substances that are composite of two or more elements. Aluminum alloy is the alloys that mainly consist of element aluminum. Aluminum alloy has many series like 7475 aluminum alloy, 2024 aluminum alloy, 5083 aluminum alloy, and 2319 aluminum alloy (see Figure 24). Aluminum alloys are lightweight materials, and they have higher corrosion resistance, oxidation resistance, good electrical and thermal conductivities, and a low-cost nature. Although they have low thermal resistance and low fatigue resistance. Aluminum alloy is a low-density alloy, it can reduce the total weight of cars or airplanes a lot, so it can improve the efficiency of cars.

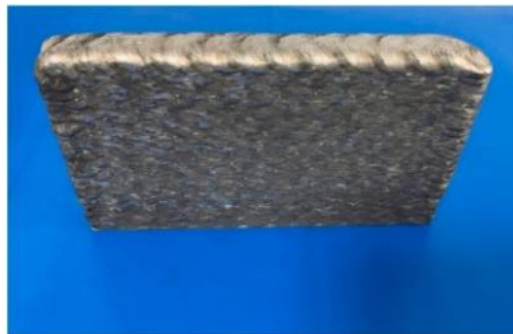


Figure 24. The shape of the additively manufactured 2319 aluminum alloy [21]

The aluminum alloys' inherent vulnerability to fatigue strength is notably aggravated when produced via additive manufacturing techniques, largely due to suboptimal surface characteristics and internal imperfections. To address this challenge, shot peening, a renowned surface enhancement method, has proven to be effective in bolstering the fatigue resistance of Al alloys. The process entails impacting the surface of a component with minute, fast-moving spherical projectiles, resulting in a multitude of improvements including the generation of compressive residual stresses, the induction of work-hardening, and microstructural alterations.

All shot peening treatments lead to a rise in surface roughness, displaying a noticeable and consistent pattern of increase as the size of the shot particles grows larger. Surprisingly, a boost in the amount of coverage achieved did not significantly elevate the roughness level (see Table 3 and Table 4).

Table 3. Surface roughness properties. Ra: average roughness; Rq: root mean square roughness; Rz: average maximum height of the profile; Rv: maximum profile valley depth, Rp: maximum profile peak height [9]

Condition	c_1 (MPa)	c_2 (MPa)	c_3	Standard deviation, S(MPa)	$\sigma_{\alpha,3*10^{-7}}$ (MPa)	Gain(%)
As-received	144	35,938	0.542	10	147	-
UFS50 100%	211	12,341	0.482	15	215	46
Z100 100%	190	846	0.215	15	211	43
Z100 1000%	197	15,450	0.498	9.9	200	36
Z425 100%	170	18,378	0.461	14	177	20
Z425+Z100	182	14,778	0.459	12	188	28

Table 4. Parameters of the five-shot peening treatments considered in this study [9]

Condition	Shot material	Bead size(mm)	Almen intensity	Coverage
UFS50 100%	steel	40 to 70	11N	100%
Z100 100%	ceramic	100 to 150	11N	100%
Z100 1000%	ceramic	100 to 150	9N	1000%
Z425 100%	ceramic	425 to 600	5A	100%
Z425+Z100	ceramic	425 to 600+100 to 150	5A+9N	100%+1000%

In general, the application of peening treatments consistently leads to an extension of the material's fatigue life. The extent of this enhancement varies according to the level of applied loads, with milder treatments, such as UFS50 100% and Z100 100%, yielding the most significant improvements. The peening treatments can improve fatigue resistance a lot, they can improve the strength of components. The fewer materials are used while maintaining the same strength, the weight decreases, so it can improve efficiency.

Currently, sectors such as aerospace, railway transportation, and defense are confronted with a pressing demand for innovative solutions that are high-performing, energy-efficient, and ultra-efficient. The lightweight nature of aluminum is instrumental in enhancing the efficiency of components across these industries. In response to these challenges, Additive Manufacturing (AM) technology has emerged as a viable solution, particularly the laser powder bed fusion (LPBF) process (see Figure 25), which boasts superior precision. The LPBF process excels in producing intricate structural components and achieving exceptional performance characteristics. Given the properties of aluminum alloys, the LPBF technology can significantly enhance their physical attributes, including specific strength.

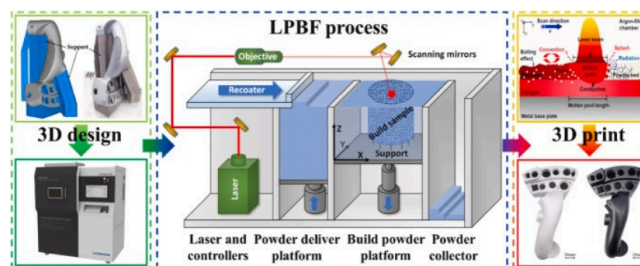


Figure 25. Schematic diagram of LPBF process

In contrast to traditionally manufactured Aluminum alloys, LPBF-produced Al-Li alloys showcase unique microstructural characteristics and more visible metallurgical bonding imperfections. The fundamental microstructural characteristics that influence the anisotropic mechanical properties of components include lamellar precipitation phases, pronounced crystallographic texturing, and the presence of columnar grains aligned parallel to the build direction. Furthermore, metallurgical imperfections such as residual stresses, porosity, cracks, and elemental depletion inevitably impede the overall forming quality of Al-Li alloys, posing significant challenges. In recent times, there has been a growing trend among researchers to delve into enhancement strategies for LPBF lightweight alloys, with a focus on achieving high isotropy and superior forming quality [22].

3. Conclusion

The use of carbon fibers, ceramics, titanium alloys, and aluminum alloys as substitutes for conventional metals in automotive components offers numerous advantages. Carbon fibers, specifically CF/PPS composites, excel in demanding automotive applications due to their superior fatigue resistance, mechanical properties, and lightweight nature, enhancing serviceability and fuel efficiency. Ceramic materials, particularly graded ceramics, exhibit higher flexural strength across all thermal shock temperature differences compared to homogeneous ceramics. Titanium alloys, such as Ti6Al4V treated with the combined USRP-PEO technology, demonstrate significantly improved fatigue resistance over PEO samples alone, with a 14-fold increase in fatigue life at 600 MPa when coated with a 20 μm layer. Aluminum alloys, in general, benefit from various strengthening treatments that effectively increase their fatigue life, with the degree of improvement dependent on the applied load level and mild treatments showing the highest enhancement.

In conclusion, among the four materials discussed, carbon fiber composites stand out as the optimal lightweight option for enhancing vehicle fuel efficiency. Their exceptional lightweight yet high-strength characteristics enable superior tensile stress resistance per unit mass, thereby delivering the highest specific strength and fatigue resistance, making them the top choice for enhancing vehicle efficiency.

References

- [1] G. Di Blasio, R. Ianniello, C. Beatrice, F. C. Pesce, A. Vassallo, and G. Belgiorno, "Additive manufacturing new piston design and injection strategies for highly efficient and ultra-low emissions combustion given 2030 targets," *Fuel*, vol. 346, p. 128270, Aug. 2023, doi: 10.1016/j.fuel.2023.128270.
- [2] H. G. Huntington, "US gasoline response to vehicle fuel efficiency: A contribution to the direct rebound effect," *Energy Econ.*, vol. 136, p. 107655, Aug. 2024, doi: 10.1016/j.eneco.2024.107655.
- [3] Z. Zhong, W. Hu, and X. Zhao, "Rethinking electric vehicle smart charging and greenhouse gas emissions: Renewable energy growth, fuel switching, and efficiency improvement," *Appl. Energy*, vol. 361, p. 122904, May 2024, doi: 10.1016/j.apenergy.2024.122904.
- [4] J. Kim, "Vehicle fuel-efficiency choices, emission externalities, and urban sprawl," *Econ. Transp.*, vol. 5, pp. 24–36, Mar. 2016, doi: 10.1016/j.ecotra.2015.10.001.
- [5] G. F. de M. Morgado, L. S. Montagna, R. F. Gouvêa, A. Guimarães, F. R. Passador, and M. C. Rezende, "Fatigue resistance of carbon fiber/polyphenylene sulfide composites engineered for automotive use," *Polym. Compos.*, vol. 45, no. 9, Art. no. 9, Jun. 2024, doi: 10.1002/pc.28299.
- [6] J.-M. Tiemann, J. Mola, P. Land, T. Krumpholz, and U. Krupp, "Quasi Static and Fatigue Properties of Long Carbon Fiber Reinforced Polyamide," *J. Mater. Eng. Perform.*, vol. 31, no. 1, Art. no. 1, Jan. 2022, doi: 10.1007/s11665-021-06182-5.
- [7] S. D. Heintze et al., "Fatigue resistance of all-ceramic fixed partial dentures – Fatigue tests and finite element analysis," *Dent. Mater.*, vol. 34, no. 3, pp. 494–507, Mar. 2018, doi: 10.1016/j.dental.2017.12.005.

- [8] C. Tan, Q. Sun, G. Zhang, and Y. Zhao, "Remarkable increase in high-cycle fatigue resistance in a titanium alloy with a fully lamellar microstructure," *Int. J. Fatigue*, vol. 138, p. 105724, Sep. 2020, doi: 10.1016/j.ijfatigue.2020.105724.
- [9] M. Benedetti, M. Pedranz, V. Fontanari, C. Menapace, and M. Bandini, "Enhancing plain fatigue strength in aluminum alloys through shot peening: Experimental investigations and a strain energy density interpretation," *Int. J. Fatigue*, vol. 184, p. 108299, Jul. 2024, doi: 10.1016/j.ijfatigue.2024.108299.
- [10] S. Wang, T. Yu, Z. Pang, X. Liu, C. Shi, and N. Du, "Improving the fatigue resistance of plasma electrolytic oxidation coated titanium alloy by ultrasonic surface rolling pretreatment," *Int. J. Fatigue*, vol. 181, p. 108157, Apr. 2024, doi: 10.1016/j.ijfatigue.2024.108157.
- [11] R. Narasimman, S. Vijayan, and K. Prabhakaran, "Carbon-carbon composite foams with high specific strength from sucrose and milled carbon fiber," *Mater. Lett.*, vol. 144, pp. 46–49, Apr. 2015, doi: 10.1016/j.matlet.2015.01.016.
- [12] Y.-J. Huang, C.-H. Wang, Y.-L. Huang, G. Guo, and S. R. Nutt, "Enhancing specific strength and stiffness of phenolic microsphere syntactic foams through carbon fiber reinforcement," *Polym. Compos.*, vol. 31, no. 2, Art. no. 2, Feb. 2010, doi: 10.1002/pc.20795.
- [13] E. E. Klu, J. Jiang, G. Wang, B. Gao, A. Ma, and D. Song, "Achieving ultrahigh specific strength of an ultrafine grained Mg–9Li–1Al alloy via the combined processing of ECAP with repeated annealing and rolling," *J. Mater. Res. Technol.*, vol. 25, pp. 3228–3242, Jul. 2023, doi: 10.1016/j.jmrt.2023.06.108.
- [14] Y. Wang et al., "Effect of short carbon fiber content on strength and toughness of Al₂O₃–C refractories," *Int. J. Appl. Ceram. Technol.*, vol. 21, no. 1, pp. 427–437, Jan. 2024, doi: 10.1111/ijac.14516.
- [15] Y. Wang, A. Li, S. Zhang, B. Guo, and D. Niu, "A review on new methods of recycling waste carbon fiber and its application in construction and industry," *Constr. Build. Mater.*, vol. 367, p. 130301, Feb. 2023, doi: 10.1016/j.conbuildmat.2023.130301.
- [16] X. Li, M. Kim, and W. Zhai, "Ceramic microlattice and epoxy interpenetrating phase composites with simultaneous high specific strength and specific energy absorption," *Mater. Des.*, vol. 223, p. 111206, Nov. 2022, doi: 10.1016/j.matdes.2022.111206.
- [17] G. Zheng, J. Zhao, C. Jia, X. Tian, Y. Dong, and Y. Zhou, "Thermal shock and thermal fatigue resistance of SiAlon–Si₃N₄ graded composite ceramic materials," *Int. J. Refract. Met. Hard Mater.*, vol. 35, pp. 55–61, Nov. 2012, doi: 10.1016/j.ijrmhm.2012.04.003.
- [18] Y. Zhang et al., "High-strength, 3D interconnected alumina ceramic foams with high porosity comparable to aerogels," *Ceram. Int.*, vol. 49, no. 23, Part B, pp. 39070–39075, Dec. 2023, doi: 10.1016/j.ceramint.2023.09.244.
- [19] P. Nyamekye, S. Rahimpour Golroudbary, H. Piili, P. Luukka, and A. Kraslawski, "Impact of additive manufacturing on titanium supply chain: Case of titanium alloys in automotive and aerospace industries," *Adv. Ind. Manuf. Eng.*, vol. 6, p. 100112, May 2023, doi: 10.1016/j.aime.2023.100112.
- [20] X. Shi, Q. Zhang, Z. Jing, Z. Fan, J. Liu, and J. Qiao, "Strengthening behavior and model of ultra-high strength Ti–15Mo–2.7Nb–3Al–0.2Si titanium alloy," *Trans. Nonferrous Met. Soc. China*, vol. 34, no. 4, pp. 1136–1149, Apr. 2024, doi: 10.1016/S1003-6326(23)66459-3.
- [21] F. Han et al., "Comparative study on corrosion property of 2219 aluminum alloy sheet and additively manufactured 2319 aluminum alloy," *J. Mater. Res. Technol.*, vol. 30, pp. 3178–3185, May 2024, doi: 10.1016/j.jmrt.2024.04.036.
- [22] L. Li, X. Meng, H. Zhang, P. Li, S. Huang, and J. Zhou, "Research status of laser powder bed fusion Al–Li alloys and its improvement measures," *J. Mater. Res. Technol.*, vol. 31, pp. 26–46, Jul. 2024, doi: 10.1016/j.jmrt.2024.06.056.